

F \cdots H–N and MeO \cdots H–N Hydrogen-Bonding in the Solid States of Aromatic Amides and Hydrazides: A Comparison Study

Yuan-Yuan Zhu, Jing Wu, Chuang Li, Jiang Zhu, Jun-Li Hou, Chang-Zhi Li, Xi-Kui Jiang, and Zhan-Ting Li*

State Key Laboratory of Bio-Organic and Natural Products Chemistry, Shanghai Institute of Organic Chemistry, Chinese Academy of Sciences, 354 Fenglin Lu, Shanghai 200032, China

Received March 15, 2007; Revised Manuscript Received May 5, 2007

ABSTRACT: Four intramolecularly F \cdots H–N hydrogen-bonded aromatic amide and hydrazide derivatives have been prepared. Their crystal structures are investigated and compared with those of their MeO \cdots H–N hydrogen-bonded analogues. It is found that all the F \cdots H–N hydrogen-bonded molecules form intermolecular C=O \cdots H–N hydrogen bonding and, for two of them, weak F \cdots H–C interactions. In contrast, the MeO \cdots H–N hydrogen-bonded molecules display only very weak intermolecular C–H \cdots π interactions. The hydrogen-bonded amide units in the fluorine-bearing molecules exhibit large torsion from the connecting benzene units. This has been attributed to the weaker ability of fluorine as a hydrogen-bonding acceptor, its smaller size (relative to the MeO group), and consequently the strengthened intermolecular NH \cdots O=C hydrogen bonding. The results also suggest that, although the weakness of fluorine as a hydrogen-bonding acceptor has been mainly attributed to its low polarizability and tightly contracted lone pairs, the great tendency of fluorine-bearing aromatic amides to form intermolecular C=O \cdots H–N hydrogen bonding may also play a role.

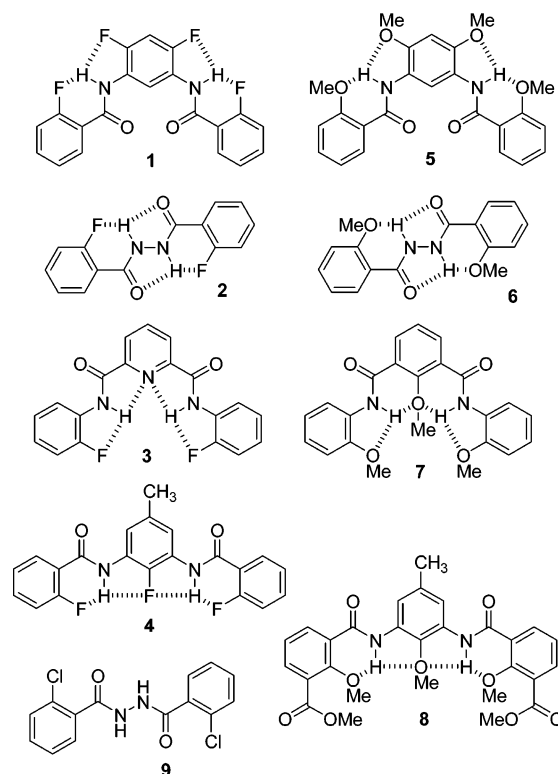
Introduction

Hydrogen bonding is one of the most useful noncovalent forces in supramolecular chemistry. In the few past decades, an ocean of literature has been devoted to hydrogen-bonding-driven self-assembly.¹ In most cases, intramolecular hydrogen bonding is used to direct rationally designed monomers to adopt preorganized shapes or conformations so that efficient intermolecular hydrogen bonding can be formed. Among the most widely used intramolecular hydrogen bonding are the O \cdots H–N and N \cdots H–N motifs.² In contrast, examples of using other heteroatoms of high negativity, such as fluorine,³ chlorine,⁴ and sulfur,⁵ as proton acceptors are very limited.

It has been well-established that the fluoride ion is a very strong proton acceptor.^{6,7} However, since the 1960s it has been proposed that covalently bound fluorine is a very weak intermolecular hydrogen-bonding acceptor due to its low polarizability and tightly contracted lone pairs.⁸ We previously reported that stable intramolecular five- or six-membered F \cdots H–N hydrogen bonding exists in aromatic amides or their oligomers in both solution and solid state.^{3a,b} With this hydrogen-bonding motif as a driving force, we have constructed several stable duplexes and foldamers.^{3a,b} Further investigations of this F \cdots H–N hydrogen-bonding motif may have fundamental importance in finding new factors that affect intra- and intermolecular interaction patterns⁹ and future design of new folded and assembling architectures. Our previous studies have focused on the three-center hydrogen bonding in the induction of folded or extended secondary structures.¹⁰ In a like manner, we have prepared four new fluorine-bearing aromatic amide and hydrazide derivatives. In this paper, we describe their crystal structures and a comparison study with their MeO \cdots H–N hydrogen-bonded analogues.

Results and Discussion

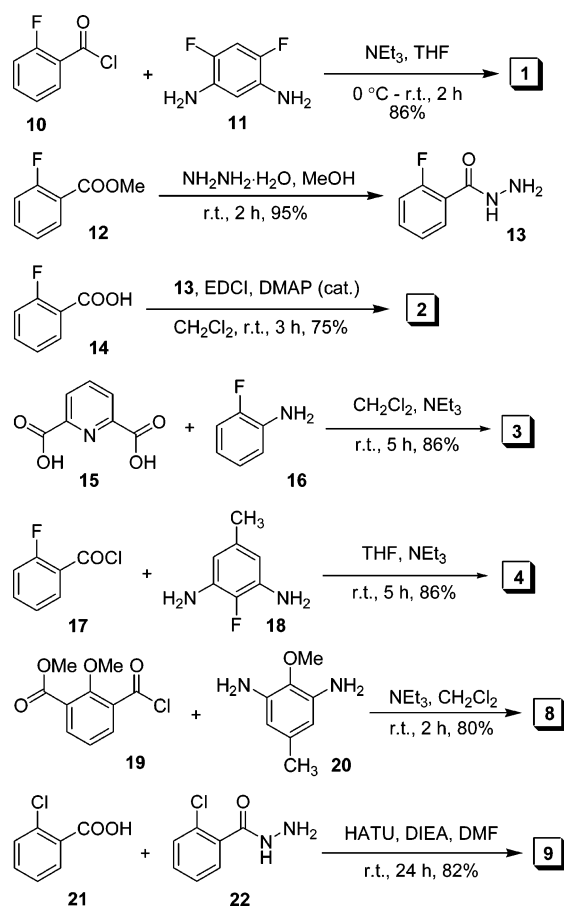
A number of fluorine-containing aromatic amides were prepared. Successfully, for four of them, that is, compounds



1–4, crystals suitable for X-ray analysis were grown by slow evaporation of their solution in chloroform at room temperature. Their crystal structures were therefore investigated and compared with those of their analogues **5–8**. The structures of compounds **5–7** have been briefly described in reported works.^{10a,c,h} The synthetic routes for compounds **1–4**, **8**, and **9** are presented in 1. It has been reported that chlorine may be a weak proton acceptor.^{4,11} For the sake of comparison, compound **9**,¹² an analogue to **1**, was also prepared. Compounds **1–4** and **8** are soluble in solvents of low polarity, such as chloroform and dichloromethane, whereas dichloride **9** is soluble only in polar solvents such as methanol and dimethyl sulfoxide. As

* Corresponding author. E-mail: ztli@mail.sioc.ac.cn.

Scheme 1



expected, the signals of the amide protons of **1–4** and **8** in the ^1H NMR spectrum of their CDCl_3 solution appeared in the downfield area (see Supporting Information), indicating the existence of intramolecular hydrogen bonding. Diluting the solution of these compounds in CDCl_3 from 20 to 0.2 mM did not cause salient shifting ($\Delta\delta \leq 0.04$ ppm) of the amide or aromatic protons. This result shows that no important aromatic stacking or intermolecular hydrogen-bonding exists in chloroform.

Table 1 lists the crystal data and structure refinements for compounds **1–9**. The crystal structures of **1** and **5** are provided in Figure 1 and their packing structures are shown in Figure 2. It can be found that the values of the four torsion angles of **1** are all significantly higher than the corresponding values of **5**.¹³ Nevertheless, the three benzene units of **1** still form a rigidified “V”-styled conformation with a backbone angle of 89.64° .¹⁴ The structure relates to a triclinic space group $P\bar{1}$, and the unit cell contains two molecules that form a dimeric structure through two intermolecular $\text{C}=\text{O}\cdots\text{H}-\text{N}$ hydrogen bonds (bonding distance: 2.488 \AA) (Figure 2a). Between the neighboring molecules within the same packing layer is a weak $\text{F}\cdots\text{H}-\text{C}$ interaction.¹⁵ The $\text{F}\cdots\text{H}$ distance is 2.428 \AA , which is about 10% shorter than the sum of the van der Waals radii (2.67 \AA). For compound **5** (Figure 1b), the largest torsion angle for the amide units is about 23.36° , which is considerably smaller than that observed for **1**. The backbone angle formed by the three benzene units is 88.94° , which is very close to that of **1**. These results show that both compounds possess comparable backbones due to the formation of four intramolecular hydrogen bonds. However, **5** displayed a staggered packing pattern (Figure 2b), which is completely different from that of **1**. In addition, no intermolecular $\text{C}=\text{O}\cdots\text{H}-\text{N}$ hydrogen-bonding or $\text{MeO}\cdots$

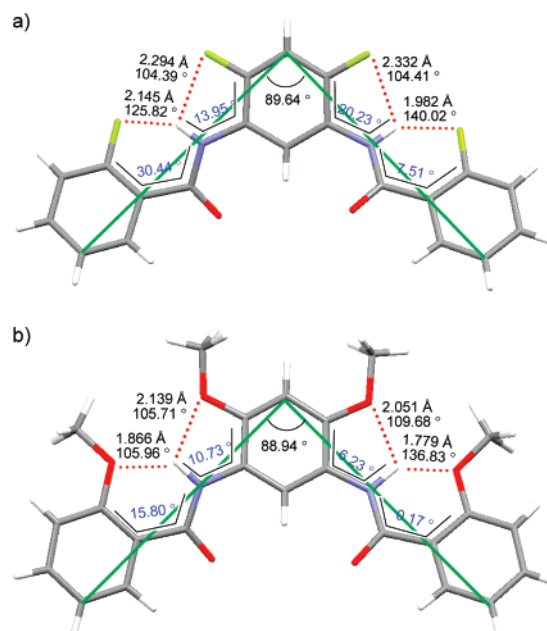


Figure 1. The crystal structures of (a) **1** and (b) **5** and the related values of the bond distances and angles.

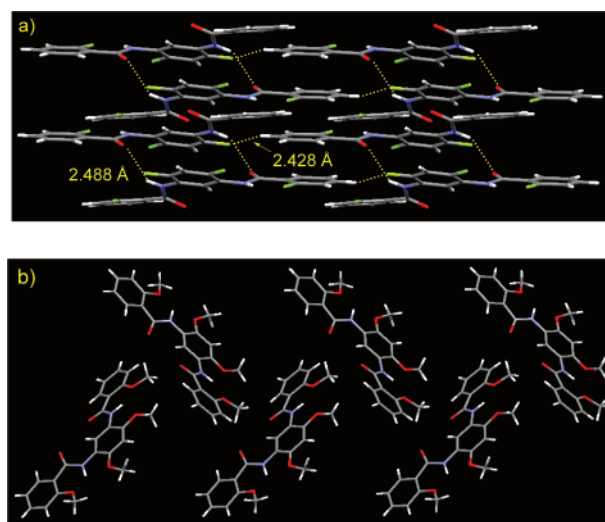


Figure 2. Packing patterns of (a) **1** and (b) **5**. The former exhibits important intermolecular hydrogen bonding and $\text{F}\cdots\text{H}-\text{C}$ interaction.

$\text{H}-\text{C}$ interaction was exhibited.¹⁶ These differences clearly show the great influence of the spatial hindrance of the MeO groups in **5** on the packing pattern. Such a hindrance prevents any intermolecular hydrogen bonding, as is observed in other $\text{MeO}\cdots\text{H}-\text{N}$ hydrogen-bonded structures.^{10a-c}

Both **2** and **6** form two intramolecular hydrogen bonds (Figures 3 and 4). The central planar hydrazide unit in **2** is pronouncedly deviated from the aromatic rings, with a torsion angle of 29.71° . In contrast, the backbone of **6** is much close to a plane (torsion angle: 5.48°). Similar to that observed for **1**, the hydrazide unit of **2** forms intermolecular $\text{C}=\text{O}\cdots\text{H}-\text{N}$ hydrogen bonding, leading to an extended layer packing (Figure 4a). Compound **6** displays a complicated staggered packing pattern (orthorhombic). No intermolecular hydrogen bonding was observed for its hydrazide unit. Instead, a relatively strong $\text{C}=\text{O}\cdots\text{H}-\text{C}(5)$ interaction and a weak $\text{C}(5)-\text{H}\cdots\pi$ interaction¹⁷ were observed, which are shown in Figure 4b. These observations, together with the above results of **1** and **5**, seem to suggest

Table 1. X-ray Data Collection and Structure Analysis Details for Compounds 1–9

	compd 1	compd 2	compd 3	compd 4	compd 5
empirical formula	C ₂₀ H ₁₂ F ₄ N ₂ O ₂	C ₁₄ H ₁₀ F ₂ N ₂ O ₂	C ₁₉ H ₁₃ F ₂ N ₃ O ₂	C ₂₁ H ₁₅ F ₃ N ₂ O ₂	C ₂₄ H ₂₄ N ₂ O ₆
formula weight	388.32	276.24	353.32	384.35	436.45
crystal system	triclinic	monoclinic	monoclinic	triclinic	monoclinic
space group	<i>P</i> $\bar{1}$	<i>P</i> 2 ₁ / <i>c</i>	<i>P</i> 2 ₁ / <i>n</i>	<i>P</i> $\bar{1}$	<i>P</i> 2 ₁ / <i>n</i>
<i>a</i> (Å)	7.570	4.782	14.384	4.830	8.091
<i>b</i> (Å)	8.418	6.948	4.975	12.954	13.681
<i>c</i> (Å)	13.544	18.366	22.709	14.672	20.184
α (deg)	82.489	90	90	105.165	90
β (deg)	75.873	93.863	102.085	90.387	96.903
γ (deg)	84.660	90	90	97.674	90
<i>V</i> (Å ³)	828.11	608.82	1589.2	877.3	2218.1
<i>Z</i>	2	2	4	2	4
<i>D</i> _{calcd} (g/cm ³)	1.557	1.507	1.477	1.455	1.307
abs coeff (mm ^{−1})	0.132	0.123	0.114	0.116	0.095
temperature (K)	293	293	293	293	293
GOF	1.007	1.003	1.009	1.092	1.021
final <i>R</i> ₁ , <i>wR</i> ₂ (<i>I</i> > 2 σ (<i>I</i>))	0.0416, 0.0890	0.0448, 0.1171	0.0628, 0.1613	0.0610, 0.1781	0.0470, 0.0846

	compd 6	compd 7	compd 8	compd 9
empirical formula	C ₁₆ H ₁₆ N ₂ O ₄	C ₂₃ H ₂₂ N ₂ O ₅	C ₂₈ H ₂₈ N ₂ O ₉	C ₁₄ H ₁₀ Cl ₂ N ₂ O ₂
formula weight	300.31	406.43	536.52	309.14
crystal system	orthorhombic	orthorhombic	monoclinic	triclinic
space group	<i>Pbca</i>	<i>Pbca</i>	<i>P</i> 2 ₁ / <i>c</i>	<i>P</i> $\bar{1}$
<i>a</i> (Å)	13.811	13.735	18.588	4.812
<i>b</i> (Å)	7.156	16.899	7.356	6.152
<i>c</i> (Å)	15.092	17.643	20.905	11.728
α (deg)	90	90	90	88.794
β (deg)	90	90	114.532	81.757
γ (deg)	90	90	90	88.045
<i>V</i> (Å ³)	1491.7	4095.0	536.52	343.40
<i>Z</i>	4	8	4	1
<i>D</i> _{calcd} (g/cm ³)	1.337	1.318	1.371	1.495
abs coeff (mm ^{−1})	0.097	0.094	0.103	0.474
temperature (K)	293	293	293	293
GOF	1.002	1.006	1.083	1.063
final <i>R</i> ₁ , <i>wR</i> ₂ (<i>I</i> > 2 σ (<i>I</i>))	0.0482, 0.0954	0.0459, 0.1053	0.0463, 0.1393	0.0545, 0.1397

that the amide or hydrazide units of molecules with intramolecular F \cdots H–N hydrogen bonding are able to form intermolecular C=O \cdots H–N hydrogen bonding, whereas similar molecules with intramolecular MeO \cdots H–N hydrogen bonding do not possess this capacity. Because other related molecules also exhibit similar stacking tendency in the crystals,^{3b,10a–c} these phenomena appear to be general for these two classes of aromatic compounds (vide infra).

Two factors may contribute to the result that the torsion angles displayed in **1** and **2** are considerably larger than those of their analogues **5** and **6**. The first is obviously because the MeO \cdots H–N hydrogen bonding is stronger than the F \cdots H–N hydrogen bonding and is able to induce a more compact rigidified

conformation (vide infra).^{18,19} Another factor should be the formation of the intermolecular C=O \cdots H–N hydrogen bonding for the fluorine-bearing molecules, which is facilitated by both the weakness of the F \cdots H–N hydrogen bonding and the substantially smaller size of fluorine relative to the MeO group (vide infra).

Numerous attempts to crystallize the 2-fluoroisophthalamide-based analogues of **3** were unsuccessful. As an adaptation, compound **3** was prepared. Its crystal structure and associated data are provided in Figure 5a. Similar to **7** (Figure 5b), there are also four intramolecular hydrogen bonds in **3**. Again, the deviation of both amide units from the fluorine-bearing benzene units is larger than that observed for the corresponding amide units of **7**. Different from **1** and **3** in that both of their amide units are involved in intermolecular hydrogen bonding, **5** displayed only one intermolecular hydrogen bond in the packing map (Figure 6a), which is formed through deviation of one amide unit from the central pyridine plane. The neighboring stacking layers packed alternately, which were held together through weak C–H \cdots π interactions. The crystal system of **7** was identical to that of **6** (Table 1), displaying no intermolecular hydrogen bonding. Very weak C(5)–H \cdots π interactions were also observed, as shown in Figure 6b. As expected, the backbone angle of **3** is substantially smaller than that of **7** due to the shrunk conformation of the pyridine unit.

The crystal structures of **4** and **8** are shown in Figure 7. The ester group-free analogue of **8** has been synthesized, but its crystal structure is not available yet. It can be found that one amide unit of **4** was substantially deviated from the connecting two benzene planes as a result of the formation of intermolecular C=O \cdots H–N hydrogen bonding (Figure 8a). Another NH proton

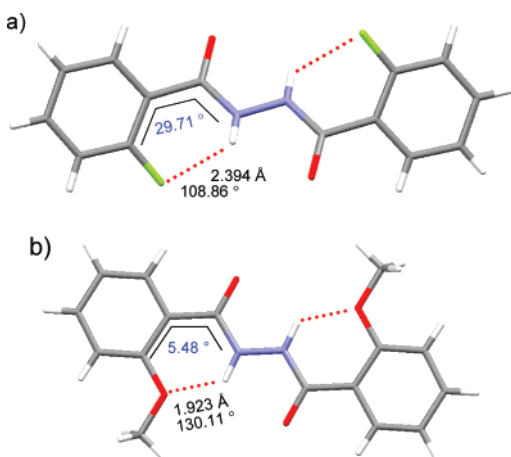


Figure 3. The crystal structures of (a) **2** and (b) **6** and the related values of the hydrogen-bond distances and angles.

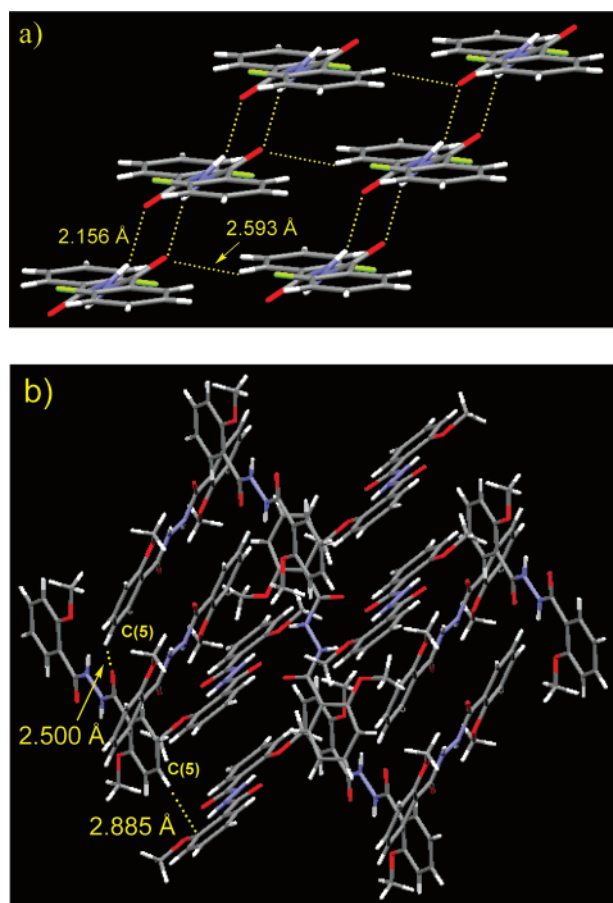


Figure 4. Packing patterns of (a) **2** and (b) **6**. The former exhibits intermolecular hydrogen bonding and $\text{C}=\text{O}\cdots\text{H}-\text{C}$ interaction, whereas the latter only forms weak intermolecular $\text{C}=\text{O}\cdots\text{H}-\text{C}$ and $\text{C}-\text{H}\cdots\pi$ interactions.

in **4** was hydrogen bonded to the two neighboring fluorine atoms but did not form intermolecular hydrogen bonding, probably due to a steric hindrance effect. Within the same packing layer, important $\text{F}\cdots\text{H}-\text{C}$ interactions were revealed (Figure 8b), leading to the formation of a dimeric structure, as revealed in the related hydrogen-bonded dimers.^{10e} Between the dimeric units significant $\text{C}=\text{O}\cdots\text{H}-\text{C}$ interactions also existed. These weak interactions, together with the four intramolecular hydrogen bonds, induced the formation of an extended supramolecular network. In contrast, no intermolecular $\text{C}=\text{O}\cdots\text{H}-\text{N}$ hydrogen bonding or other weak interactions were observed for compound **8** (Figure 8c). The $\pi-\pi$ stacking interaction is the main driving force for the intermolecular packing.

Figure 9 shows the crystal structure of dichloride **9**. Both amide groups of the molecule were involved in intermolecular hydrogen bonding. This is similar to that observed for its counterpart **2**. However, no intramolecular $\text{Cl}\cdots\text{H}-\text{N}$ hydrogen bonding was formed. Actually, the electronegative chlorine and carbonyl oxygen atoms were oriented at the same side of the backbone. The result shows that the chlorines in this molecule were unable to form intramolecular six-membered hydrogen bonding, although an IR study in solution showed evidence for the existence of intramolecular five-membered $\text{Cl}\cdots\text{H}-\text{N}$ hydrogen bonding in *N*-(*o*-chlorophenyl)urea derivatives.^{4a} The torsion angle of the amide is 46.51° , which is substantially larger than that observed for **2**. As a result, the intermolecular hydrogen bonding in this molecule is remarkably stronger (with a considerably shorter $\text{O}\cdots\text{H}$ distance, Figure 9) than that formed by **2**. This result also excludes the possibility that the intramo-

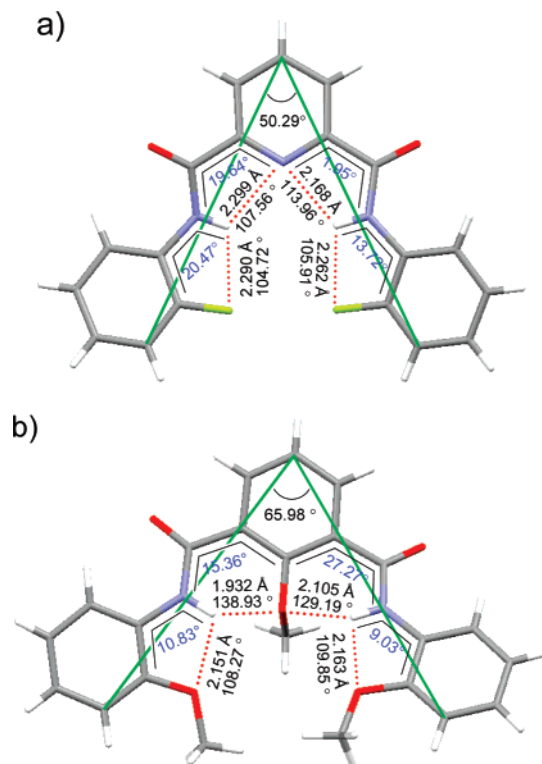


Figure 5. The crystal structures of (a) **3** and (b) **7** and the related values of the bond distances and angles.

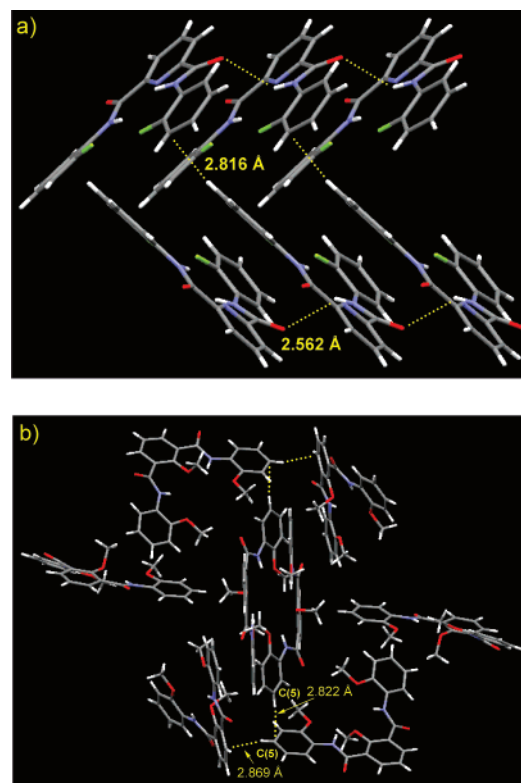


Figure 6. Packing patterns of (a) **3** and (b) **7**. The former exhibits one intermolecular hydrogen bonding and $\text{C}-\text{H}\cdots\pi$ interaction, whereas the latter shows only two weak intermolecular $\text{C}-\text{H}\cdots\pi$ interactions.

lecular $\text{F}\cdots\text{H}-\text{N}$ hydrogen bonding was driven by the electrostatic repulsion of the electronegative fluorine and carbonyl oxygen atoms.

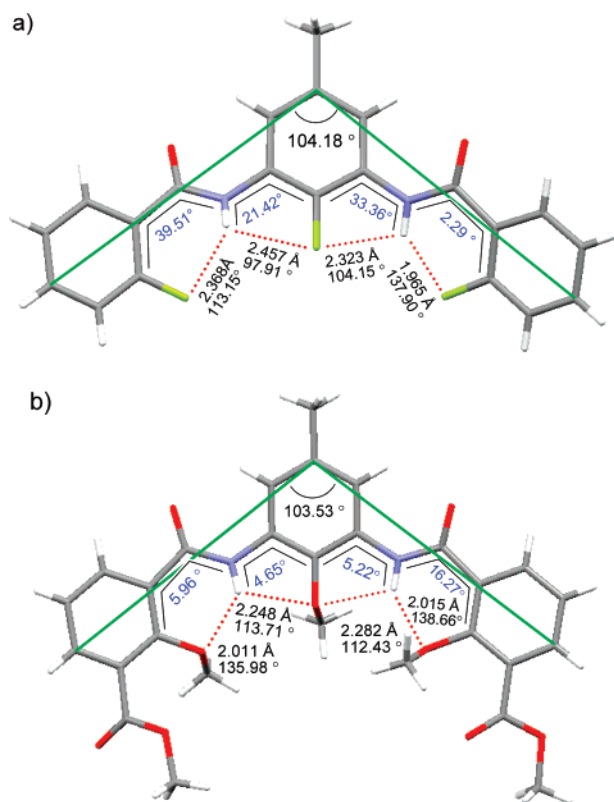


Figure 7. The crystal structures of (a) **4** and (b) **8** and the related values of the bond distances and angles.

Theoretically, the shorter the distance is between a hydrogen-bonding heteroatom acceptor and the associated proton, the stronger the corresponding hydrogen bonding will be.¹⁸ A comparison of the ratio of such distances and the sum of the van der Waals radii of the related heteroatom and hydrogen may provide deeper insight into the relative stability of the hydrogen bonding.¹⁹ The corresponding values for compounds **1–8** are listed in Table 2. Generally, a smaller value means shorter heteroatom–hydrogen contact and higher bonding stability. Because of the difference in molecular backbones or the existence of additional groups, it may be unreasonable to compare the values of **3** and **4** with those of **7** and **8**. Nevertheless, comparing the values of **1** and **2** with those of their backbone-identical analogues **5** and **6** reveals that the extent of the shortening in the contacts for **5** and **6** was generally larger than that of **1** and **2**. One obvious factor for causing this difference should be that the capacity of oxygen as a hydrogen-bonding acceptor is stronger than that of fluorine. Because intermolecular $\text{C}=\text{O}\cdots\text{H}-\text{N}$ hydrogen-bonding persists for all the fluorine-bearing compounds **1–4**, this intermolecular bonding should also play a role in inducing the larger torsion of the amide unit from the connecting benzene plane and consequently increasing the distance of the fluorine from the bonded proton. Direct evidence to support this interaction comes from the crystal structure of **23** (Figure 10).^{3b} Because of the existence of the large triphenylmethyl group, the amide unit of this molecule did not form intermolecular hydrogen bonding. As a result, the distances between the two fluorine atoms and the amide proton are considerably shorter than the corresponding values of **1–4**.

Summary and Conclusions

The crystal structures of eight $\text{F}\cdots\text{H}-\text{N}$ and $\text{MeO}\cdots\text{H}-\text{N}$ hydrogen-bonded aromatic amides and hydrazides have been

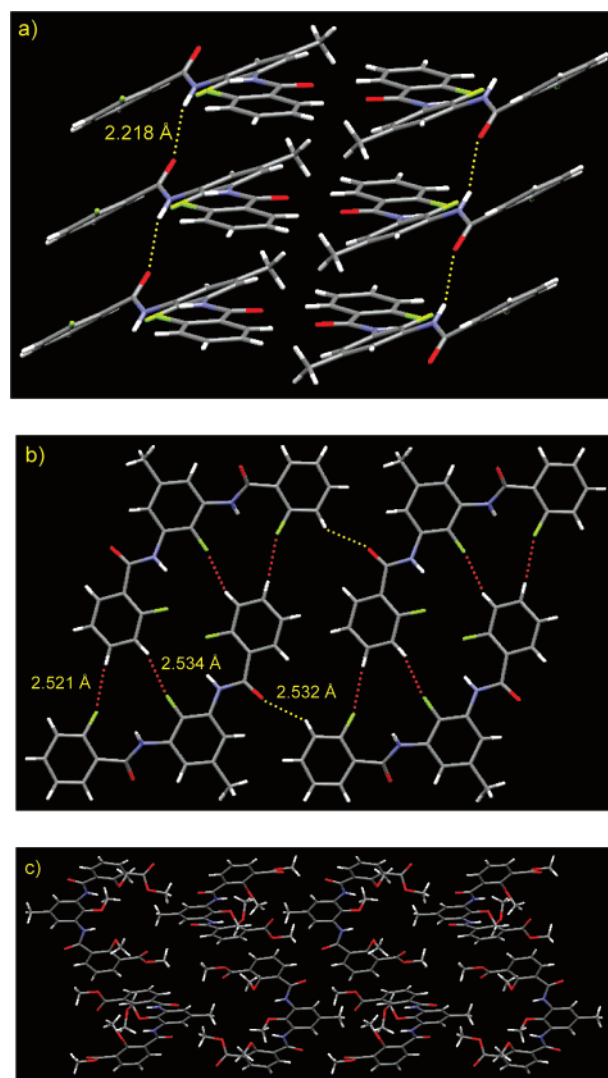


Figure 8. Packing patterns of (a) **4** (view from the *b*-axis), (b) **4** (view from the *c*-axis) and (c) **8**. The former exhibits intermolecular hydrogen bonding, $\text{C}-\text{H}\cdots\text{F}$ and $\text{C}-\text{H}\cdots\text{O}=\text{C}$ interactions.

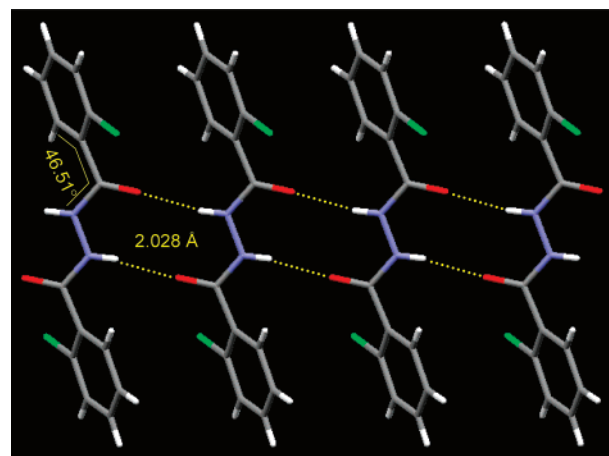


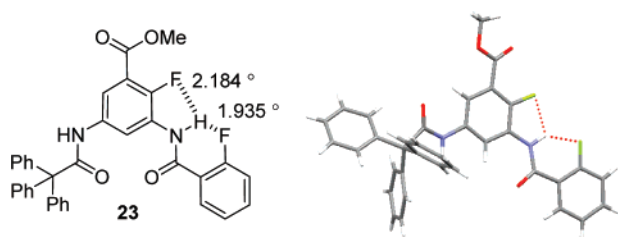
Figure 9. The crystal structure of **9**, which reveals a large torsion angle for the amide units and intermolecular $\text{C}=\text{O}\cdots\text{H}-\text{N}$ hydrogen bonding but no intramolecular six-membered $\text{C}=\text{O}\cdots\text{H}-\text{N}$ hydrogen bonding.

investigated and compared. It is revealed that, although the $\text{F}\cdots\text{H}-\text{N}$ hydrogen bonding is weaker than the $\text{MeO}\cdots\text{H}-\text{N}$ hydrogen bonding of the same motif, the smaller size of fluorine

Table 2. Ratio of the Distances between the Hydrogen-Bonded Heteroatom and the Related Proton and the Sum of Their Van Der Waals Radii^a

compd	five-membered		six-membered		compd	five-membered		six-membered	
1	0.859	0.875	0.803	0.742	5	0.786	0.754	0.686	0.654
2			0.897		6			0.710	
3	0.861	0.811			7	0.791	0.795	0.710	0.774
	0.858	0.847			8	0.826	0.839	0.739	0.741
4	0.920	0.870	0.884	0.736					

^a The van der Waals radii of fluorine, oxygen, and hydrogen are 1.47, 1.52, and 1.20 Å, respectively.²⁰

**Figure 10.** Compound **23** and its crystal structure.

relative to the MeO group has great influence on the stacking patterns of their derivatives in the solid state. For the F...H-N hydrogen-bonded molecules, intermolecular C=O...H-N hydrogen bonding and, in some cases, F...H-C interactions have been revealed. In contrast, their MeO...H-N hydrogen-bonded analogues can generate only weak intermolecular interactions due to the increased steric bulk of the MeO group.

Traditionally, the weakness of fluorine as a hydrogen-bonding acceptor has been attributed to its low polarizability and tightly contracted lone pairs; the present study has revealed a new factor, that is, the great tendency of fluorine-bearing derivatives to form intermolecular C=O...H-N hydrogen bonding as a result of the feature of its small size. Obviously, this factor should be carefully considered in the future design of F...H-N hydrogen-bonding-driven structural materials. The chlorine-substituted analogue also displays similar intermolecular hydrogen bonding. Considering the increasing interest in weak hydrogen bonding or halogen bonding in recent years,²¹ it should be of importance to rationally avoid or utilize such intermolecular interaction for new crystal and materials design.

Previous studies have revealed that fluorine in some aromatic amides could form intermolecular F...H-N hydrogen bonding with ammonium protons.^{3b,c} Therefore, a logic extension of the present study is to explore whether similar intermolecular hydrogen-bonding forms between fluorine and neutral amide or amino protons. The feature of the small size of fluorine may also be utilized to construct tube-styled supramolecular structures from F...H-N hydrogen-bonded folded aromatic oligoamides. Preliminary investigation has shown that strong π - π stacking exists between F...H-N hydrogen-bonded folded aromatic oligoamides and fullerenes, which may find applications in new materials design.

Experimental Section

General Procedures. See Supporting Information.

Compound 1. To a solution of diamine **11**²² (0.052 g, 0.36 mmol) and triethylamine (0.80 mL, 8.00 mmol) in tetrahydrofuran (THF) (20 mL), cooled in an ice-bath, was added a solution of acyl chloride **10** (0.13 g, 0.82 mmol) in THF (10 mL). The solution was stirred at room temperature for 3 h and then washed with dilute hydrochloric acid (1 N, 15 mL \times 2), saturated sodium bicarbonate solution (15 mL), water (15 mL), and brine (15 mL) and dried over sodium sulfate. After the solvent was removed under reduced pressure, the resulting residue was subjected to column chromatography (*n*-hexane/EtOAc 15:1) to give compound **1** as a white solid (0.060 g, 86%). mp 220–222 °C.

¹H NMR (CDCl₃): δ 9.41 (t, J = 8.2 Hz, 1 H), 8.64 (d, J = 16.2 Hz, 2 H), 8.23 (t, J_1 = 8.0 Hz, J_2 = 1.8 Hz, 2 H), 7.59–7.51 (m, 2 H), 7.33 (t, J = 7.5 Hz, 2 H), 7.26–7.17 (m, 2 H), 7.02 (t, J = 10.2 Hz), 1.3C NMR (CDCl₃): δ 162.2, 161.1, 158.9, 134.1, 132.6, 125.2, 122.4, 120.7, 117.4, 116.2, 103.4. ¹⁹F NMR (CDCl₃): δ -112.8 to -112.99 (m, 1 F), -129.4 (t, J = 9.8 Hz). MS (ESI): m/z 389 [M + H]⁺. HRMS (ESI): Calcd. for C₂₀H₁₃N₂O₂F₄ [M]⁺: 389.0908. Found: 389.0909.

Compound 13. A solution of ester **12** (1.00 g, 6.49 mmol) and hydrazine hydrate (1.60 mL, 32.5 mmol) in methanol was stirred at room temperature for 2 h and then concentrated under reduced pressure. The resulting residue was washed with cold water, dried, and then subjected to column chromatography (CH₂Cl₂/AcOEt 4:1) to give compound **13**²³ as a white solid (0.95 g, 95%). mp 72–73 °C. ¹H NMR (CDCl₃): δ 8.06 (t, d, J_1 = 7.5 Hz, J_2 = 1.8 Hz, 1 H), 8.04 (br, 1 H), 7.51–7.43 (m, 1 H), 7.25 (t, J = 7.5 Hz, 1 H), 7.11 (d, J_1 = 12.0 Hz, J_2 = 8.1 Hz, 1 H), 4.09 (br, 2 H). ¹³C NMR (CDCl₃): δ 161.9, 159.0, 134.3, 132.0, 125.1, 116.4, 116.1. ¹⁹F NMR (CDCl₃): δ -112.1 (s, 1 F). MS (ESI): m/z 155.1 [M + H]⁺. Anal. Calcd. for C₇H₇FN₂O: C, 54.54; H, 4.58; N, 18.17. Found: C, 54.70; H, 4.70; N, 18.24.

Compound 2. A solution of **13** (0.16 g, 1.07 mmol), **14** (0.15 g, 1.07 mmol), EDCI (0.30 g, 1.60 mmol), and DMAP (0.01 g) in dichloromethane (15 mL) was stirred at room temperature for 3 h, and then another portion of dichloromethane (25 mL) was added. The solution was washed with saturated sodium bicarbonate solution (20 mL), water (15 mL \times 3), and brine (15 mL) and dried over sodium sulfate. After the solvent was removed under reduced pressure, the resulting residue was purified by column chromatography (CH₂Cl₂/AcOEt 15:1) to give compound **2** as a white solid (0.22 g, 75%). mp 193–194 °C. ¹H NMR (CDCl₃): δ 9.81 (d, J = 9.3 Hz, 2 H), 8.14 (t, J = 7.8 Hz, 2 H), 7.55 (d, J_1 = 14.3 Hz, J_2 = 6.9 Hz, 2 H), 7.31 (t, J = 7.5 Hz, 2 H), 7.20 (d, J_1 = 12.2 Hz, J_2 = 8.1 Hz, 2 H). ¹³C NMR (CDCl₃): δ 161.9, 159.0, 134.3, 132.0, 125.1, 116.4, 116.1. ¹⁹F NMR (CDCl₃): δ -111.00–111.12 (m, 2 F). MS (ESI): m/z 277 [M + H]⁺. Anal. Calcd. for C₁₄H₁₀F₂N₂O₂: C, 60.87; H, 3.65; N, 10.14. Found: C, 60.77; H, 3.68; N, 10.11.

Compound 3. A solution of pyridine-2,6-dicarboxylic acid (0.84 g, 5.00 mmol) in oxalyl chloride (1.50 mL, 18.6 mmol) and dimethylformamide (DMF) (0.05 mL) was stirred at room temperature for 30 min and then concentrated under reduced pressure. The resulting product **15** was dissolved in dichloromethane (10 mL). The solution was added to a stirred solution of **16** (0.96 mL, 10.0 mmol) and triethylamine (1.80 mL, 13.0 mmol) in dichloromethane (15 mL). Stirring was continued at room temperature for 3 h, and the solution was washed with saturated sodium bicarbonate solution (15 mL), water (15 mL), and brine (15 mL) and dried over sodium sulfate. Upon removal of the solvent in vacuo, the resulting residue was subjected to column chromatography (chloroform/AcOEt 20:1) to give compound **3** as a white solid (1.52 g, 86%). mp 236–237 °C. ¹H NMR (CDCl₃): δ = 10.07 (s, 2 H), 8.68–8.63 (m, 2 H), 8.56 (d, J = 7.8 Hz, 2 H), 8.22 (t, J = 7.8 Hz, 1 H), 7.24–7.13 (m, 6 H). ¹³C NMR (CDCl₃): δ 160.6, 154.4, 151.1, 148.6, 139.9, 126.1, 125.7, 124.8, 120.9, 115.0. MS (EI) m/z : 353 [M]⁺. Anal. Calcd. For C₁₉H₁₃F₂N₃O₂: C, 64.52; H, 3.78; N, 11.89. Found: C, 64.59; H, 3.71; N, 11.89.

Compound 4. A solution of **14** (0.10 g, 0.68 mmol) in oxalyl chloride (1.00 mL) and DMF (0.05 mL) in THF (20 mL) was stirred at room temperature for 30 min and then concentrated in vacuo. The resulting product **17** was dissolved in THF (20 mL) and then added to a solution of **18**^{3b} (50 mg, 0.34 mmol) and triethylamine (0.50 mL) in THF (20 mL). The mixture was stirred at room temperature for 3 h, and then the solvent was removed under reduced pressure. After workup, the crude product was purified by column chromatography (chloroform) to give compound **4** as a white solid (0.11 g, 82%). mp 220–222 °C. ¹H NMR (CDCl₃): δ 8.72 (d, J = 16.8 Hz, 2 H), 8.18 (d, J_1 = 7.8 Hz, J_2 = 1.5 Hz, 2 H), 8.04 (d, J = 7.2 Hz, 2 H), 7.58 –

7.50 (m, 2 H), 7.32 (d, t, $J_1 = 7.8$ Hz, $J_2 = 0.9$ Hz, 2 H), 7.20 (d, d, $J_1 = 8.4$ Hz, $J_2 = 8.4$ Hz, 2 H), 2.39 (s, 3 H). ^{13}C NMR (CDCl_3): δ 161.5, 161.1, 159.5, 134.6, 134.1, 132.3, 125.6, 125.1, 120.9, 118.1, 116.2, 21.7. ^{19}F NMR: δ -112.86 to -113.01 (m, 2 F), -150.89 (s, 1 F). MS (MALDI-TOF): m/z [$\text{M} + \text{H}$] $^+$: 385.2. Anal. Calcd. for $\text{C}_{21}\text{H}_{15}\text{F}_3\text{N}_2\text{O}_2$: C, 65.62; H, 3.93; N, 7.29. Found: C, 65.56; H, 4.19; N, 6.85.

Compound 8. To a solution of 2-methoxy-3-(methoxycarbonyl)-benzoic acid (0.63 g, 3.00 mmol) and DMF (0.05 mL) in THF (20 mL) was added dropwise oxalyl chloride (2 mL). The solution was stirred at room temperature for 30 min and then concentrated under reduced pressure. The resulting acyl chloride **19** was dissolved in dichloromethane (15 mL). The solution was added to a solution of **20**²⁴ (0.17 g, 1.50 mmol) and triethylamine (3 mL) in dichloromethane (20 mL), and the mixture was stirred at room temperature for 3 h. After workup, the resulting residue was subjected to column chromatography (chloroform/AcOEt 10:1) to afford compound **8** as a pale yellow solid (0.63 g, 80%). mp 150–152 °C. ^1H NMR (CDCl_3): δ 10.32 (s, 2 H), 8.40 (d, $J = 7.2$ Hz, 2 H), 8.17 (s, 2 H), 8.00 (d, $J = 7.2$ Hz, 2 H), 7.35 (t, $J = 7.8$ Hz, 2 H), 4.04 (s, 6 H), 3.98 (s, 6 H), 3.87 (s, 3 H), 2.41 (s, 3 H). ^{13}C NMR (CDCl_3): δ 165.8, 162.4, 158.2, 136.9, 136.2, 135.4, 135.3, 131.2, 127.9, 125.3, 124.6, 117.2, 64.0, 61.5, 52.6, 21.9. MS (MALDI-TOF): m/z 537.3 [$\text{M} + \text{H}$] $^+$. HRMS (MALDI-TOF): Calcd. For $\text{C}_{28}\text{H}_{28}\text{N}_2\text{O}_9\text{Na}$ [M] $^+$: 559.1687. Found: 559.1684. Anal. Calcd. For $\text{C}_{28}\text{H}_{28}\text{N}_2\text{O}_9$: C, 62.68; H, 5.26; N, 5.22. Found: C, 62.87; H, 5.13; N, 5.04.

Compound 9.¹² Compound **21** (0.28 g, 1.78 mmol) and HATU (0.74 g, 2.00 mmol) were dissolved in DMF (10 mL). To the solution was added a solution of **22** (0.30 g, 1.78 mmol) and diisopropylethylamine (DIEA) (3 mL) in DMF (10 mL). The solution was stirred at room temperature for 24 h, and then ether (50 mL) was added. The precipitate formed was filtered, washed with ether, and recrystallized from chloroform and methanol to give compound **9** as a white solid (0.45 g, 82%). Mp 221–223 °C. ^1H NMR (CD_3OD): δ 7.72 (d, $J = 7.5$ Hz, 2 H), 7.56–7.41 (m, 8 H). MS (ESI): m/z 309.1 [$\text{M} + \text{H}$] $^+$.

Acknowledgment. This work was financially supported by the National Natural Science Foundation (Nos. 20332040, 20425208, 20572126, 20621062, 20672137) and the National Basic Research Program (2007CB808000) of China.

Supporting Information Available: General experimental procedures; the ^1H NMR spectrum of **1–4** and **8** in chloroform- d ; the cif files of **1–4**, **8**, and **9**. This material is available free of charge via the Internet at <http://pubs.acs.org>.

References

- (1) (a) Lawrence, D. S.; Jiang, T.; Levitt, M. *Chem. Rev.* **1995**, 95, 2229. (b) Zeng, F.; Zimmerman, S. C. *Chem. Rev.* **1997**, 97, 1681. (c) Conn, M. M.; Rebek, J., Jr. *Chem. Rev.* **1997**, 97, 1647. (d) Nowick, J. S. *Acc. Chem. Res.* **1999**, 32, 287. (e) Krische, M. J.; Lehn, J.-M. *Struct. Bonding* **2000**, 96, 3. (f) Zimmerman, S. C.; Corbin, P. S. *Struct. Bonding* **2000**, 96, 63. (g) Schmuck, C.; Wienand, W. *Angew. Chem., Int. Ed.* **2001**, 40, 4363. (h) Archer, E. A.; Gong, H.; Krische, M. J. *Tetrahedron* **2001**, 57, 1139. (i) Brunsfeld, L.; Folmer, B. J. B.; Meijer, E. W.; Sijbesma, R. P. *Chem. Rev.* **2001**, 101, 4071. (j) Prins, L. J.; Reinhoudt, D. N.; Timmerman, P. *Angew. Chem., Int. Ed.* **2001**, 40, 2383. (k) Sijbesma, R. P.; Meijer, E. W. *Chem. Commun.* **2003**, 5. (l) Shenhar, R.; Rotello, V. M. *Acc. Chem. Res.* **2003**, 36, 549. (m) Ajayaghosh, A.; George, S. J.; Schenning, A. P. H. J. *Top. Curr. Chem.* **2005**, 258, 83. (n) Huang, F.; Gibson, H. W. *Prog. Polym. Sci.* **2005**, 30, 982. (o) Lukin, O.; Vögtle, F. *Angew. Chem., Int. Ed.* **2005**, 44, 1456.
- (2) (a) Gong, B. *Chem. Eur. J.* **2001**, 7, 4336. (b) Huc, I. *Eur. J. Org. Chem.* **2004**, 17. (c) Sanford, A.; Yamato, K.; Yang, X. W.; Yuan, L. H.; Han, Y. H.; Gong, B. *Eur. J. Biochem.* **2004**, 271, 1416. (d) Lockman, J. W.; Paul, N. M.; Parquette, J. R. *Prog. Polym. Sci.* **2005**, 30, 423. (e) Li, Z.-T.; Hou, J.-L.; Li, C.; Yi, H.-P. *Chem. Asian J.* **2006**, 1, 766.
- (3) (a) Zhao, X.; Wang, X.-Z.; Jiang, X.-K.; Chen, Y.-Q.; Li, Z.-T.; Chen, G.-J. *J. Am. Chem. Soc.* **2003**, 125, 15128. (b) Li, C.; Ren, S.-F.; Hou, J.-L.; Yi, H.-P.; Zhu, S.-Z.; Jiang, X.-K.; Li, Z.-T. *Angew. Chem., Int. Ed.* **2005**, 44, 5725. (c) Takemura, H.; Kon, N.; Yasutake, M.; Makashima, S.; Shinmyozu, T.; Inazu, T. *Chem. Eur. J.* **2000**, 6, 2334.
- (4) (a) Mido, Y.; Okuno, T. *J. Mol. Struct.* **1982**, 82, 29. (b) Banerjee, R.; Desiraju, G. R.; Mondal, R.; Howard, J. A. K. *Chem. Eur. J.* **2004**, 10, 3373.
- (5) (a) Ueyama, N.; Nishikawa, N.; Yamada, Y.; Okamura, T.; Nakamura, A. *J. Am. Chem. Soc.* **1996**, 118, 12826. (b) Baba, K.; Okamura, T.-a.; Yamamoto, H.; Yamamoto, T.; Ohama, M.; Ueyama, N. *Inorg. Chem.* **2006**, 45, 8365.
- (6) (a) Harrell, S. A.; McDaniel, D. H. *J. Am. Chem. Soc.* **1964**, 86, 4497. (b) Coles, S. J.; Frey, J. G.; Gale, P. A.; Hursthouse, M. B.; Light, M. E.; Navakhun, K.; Thomas, G. L. *Chem. Commun.* **2003**, 568.
- (7) (a) Pauling, L. *The Nature of the Chemical Bond*, 3rd ed.; Cornell University Press: Ithaca, New York, 1960; p 464. (b) Dietrich, B.; Lehn, J.-M.; Guilhem, J.; Pascard, C. *Tetrahedron Lett.* **1989**, 30, 4125.
- (8) (a) Howard, H. A. K.; Hoy, V. J.; O'Hagan, D.; Smith, G. T. *Tetrahedron* **1996**, 52, 12613. (b) Dunitz, J. D.; Taylor, R. *Chem. Eur. J.* **1997**, 3, 89. (c) Dunitz, J. D. *ChemBioChem* **2004**, 5, 614. (d) Takemura, H.; Kon, N.; Yasutake, M.; Nakashima, S.; Shinmyozu, T.; Inazu, T. *Chem. Eur. J.* **2000**, 6, 2334.
- (9) Etter, M. C. *Acc. Chem. Res.* **1990**, 23, 120.
- (10) (a) Hou, J.-L.; Shao, X.-B.; Chen, G.-J.; Zhou, Y.-X.; Jiang, X.-K.; Li, Z.-T. *J. Am. Chem. Soc.* **2004**, 126, 12386. (b) Wu, Z.-Q.; Jiang, X.-K.; Zhu, S.-Z.; Li, Z.-T. *Org. Lett.* **2004**, 6, 229. (c) Zhu, J.; Wang, X.-Z.; Chen, Y.-Q.; Jiang, X.-K.; Chen, X.-Z.; Li, Z.-T. *J. Org. Chem.* **2004**, 69, 6221. (d) Wu, Z.-Q.; Shao, X.-B.; Li, C.; Hou, J.-L.; Wang, K.; Jiang, X.-K.; Li, Z.-T. *J. Am. Chem. Soc.* **2005**, 127, 17460. (e) Zhu, J.; Lin, J.-B.; Xu, Y.-X.; Shao, X.-B.; Jiang, X.-K.; Li, Z.-T. *J. Am. Chem. Soc.* **2006**, 128, 12307. (f) Hou, J.-L.; Yi, H.-P.; Shao, X.-B.; Li, C.; Wu, Z.-Q.; Jiang, X.-K.; Wu, L.-Z.; Tung, C.-H.; Li, Z.-T. *Angew. Chem., Int. Ed.* **2006**, 45, 796. (g) Yi, H.-P.; Wu, J.; Ding, K.-L.; Jiang, X.-K.; Li, Z.-T. *J. Org. Chem.* **2007**, 72, 870.
- (11) (a) Ahrens, B.; Jones, P. G.; Fischer, A. K. *Eur. J. Inorg. Chem.* **1999**, 1103. (b) Shivanyuk, A.; Paulus, E. F.; Rissanen, K.; Kolehmainen, E.; Bohmer, V. *Chem.-Eur. J.* **2001**, 7, 1944.
- (12) Sailu, B.; Komaraiah, A.; Reddy, P. S. N. *Synth. Commun.* **2006**, 36, 1907.
- (13) This value is defined as the deviating extent of an amide unit from the plane of the 2-fluoro or 2-methoxybenzene unit to which it was connected and presented in blue in the figures.
- (14) We define this value by the three carbon atoms on the tops of the amide backbone, shown by the green lines in the figures, for the comparison of the influence of the fluorine and methoxyl groups on the shape of the backbones in solid state structures.
- (15) (a) Mele, A.; Vergani, B.; Viani, F.; Meille, S. V.; Farina, A.; Bravo, P. *Eur. J. Org. Chem.* **1999**, 187. (b) Ghosh, S.; Choudhury, A. R.; Row, T. N. G.; Maitra, U. *Org. Lett.* **2005**, 7, 1441.
- (16) (a) Castellano, R. K. *Curr. Org. Chem.* **2004**, 8, 845. (b) Dzierzawska-Majewska, A.; Obniska, J.; Karolak-Wojciechowska, J. *J. Mol. Struct.* **2006**, 783, 66. (c) Mirzaei, M.; Hadipour, N. L.; Ahmadi, K. *Biophys. Chem.* **2007**, 125, 411.
- (17) (a) Bürgik, H.-B.; Capelli, S. C.; Goeta, A. E.; Howard, J. A. K.; Spackman, M. A.; Yufit, D. S. *Chem.-Eur. J.* **2002**, 8, 3512. (b) Meyer, E. A.; Castellano, R. K.; Diederich, F. *Angew. Chem., Int. Ed.* **2003**, 42, 1210. (c) Mathur, Puniti; Ramakumar, S.; Chauhan, V. S. *Biopolymers* **2004**, 76, 150.
- (18) (a) Kollman, P. A.; Allen, L. C. *Chem. Rev.* **1972**, 72, 283. (b) Chen, J.; McAllister, M. A.; Lee, J. K.; Houk, K. N. *J. Org. Chem.* **1998**, 63, 4611.
- (19) Mitra, J.; Ramakrishnan, C. *Int. J. Peptide Protein Res.* **1981**, 17, 401.
- (20) Bondi, A. J. *Phys. Chem.* **1964**, 68, 441.
- (21) (a) Desiraju, G. R. *Acc. Chem. Res.* **2002**, 35, 565. (b) Wuest, J. D. *Chem. Commun.* **2005**, 5830. (c) Metrangolo, P.; Neukirch, H.; Pilati, T.; Resnati, G. *Acc. Chem. Res.* **2005**, 38, 386. (d) Datta, A.; Pati, S. K. *Chem. Soc. Rev.* **2006**, 35, 1305. (e) Reddy, C. M.; Kirchner, M. T.; Gundakaram, R. C.; Padmanabhan, K. A.; Desiraju, G. R. *Chem.-Eur. J.* **2006**, 12, 2222. (f) Metrangolo, P.; Resnati, G.; Pilati, T.; Liantonio, R.; Meyer, F. J. *Polym. Sci., Part A: Polym. Chem.* **2007**, 45, 1. (g) Dalgarno, S. J.; Thallapally, P. K.; Barbour, L. J.; Atwood, J. L. *Chem. Soc. Rev.* **2007**, 36, 236.
- (22) Kiprianov, N. *J. Org. Chem. USSR* **1972**, 8, 1730.
- (23) Li, Y.; Liu, J.; Zhang, H.; Yang, X.; Liu, Z. *Bioorg. Med. Chem. Lett.* **2006**, 16, 2278.
- (24) Cram, D. J.; Dicker, I. B.; Lauer, M.; Knobler, C. B. *J. Am. Chem. Soc.* **1984**, 106, 7150.